Dissolution Behavior and Varied Mesoporosity of Zeolites by NH4F Etching

Zhengxing Qin, Zhenchao You, Krassimir Bozhilov, Stefan Kolev, Wei Yang, Yanfeng Shen, Xin Jin, Jean-Pierre Gilson, Svetlana Mintova, Georgi Vayssilov, et al.

Dissolution behavior of zeolites leading to varied mesoporosity by NH_4F Etching

Zhengxing Qin,[a],* Zhenchao You,[a] Krassimir N. Bozhilov,[b] Stefan K. Kolev,[c] Wei Yang,[a] Yanfeng Shen,[a] Xin Jin,[a] Jean-Pierre Gilson,[d] Svetlana Mintova,[a,d] Georgi N. Vayssilov,[e],* Valentin Valtchev[d,f],*

[a] Prof. Zhengxing Qin, Zhenchao You, Wei Yang, Dr. Yanfeng Shen, Prof. Xin Jin, Prof. Svetlana Mintova,
State Key Laboratory of Heavy Oil Processing, College of Chemical Engineering,
China University of Petroleum East China - Qingdao Campus,
No. 66, West Changjiang Road, Huangdao District,
E-mail: zhengxing.qin@upc.edu.cn.

[b] Dr. Krassimir N. Bozhilov,
Central Facility for Advanced Microscopy and Microanalysis,
University of California,
Riverside 900 University Avenue, Riverside, CA 92521, USA.

[c] Prof. Stefan K. Kolev,
"E. Djakov"Institute of Electronics,
Bulgarian Academy of Sciences,
72 Tzarigradsko Chausee Blvd., 1784 Sofia, Bulgaria.

[d] Dr. Jean-Pierre Gilson, Prof. Svetlana Mintova, Prof. Valentin Valtchev,
Laboratoire Catalyse et Spectrochimie,
Normandie Univ,
ENSICAEN, UNICAEN, CNRS, 14000 Caen, France, 6 Bd Maréchal Juin, 14000 Caen, France,
E-mail: valentin.valtchev@ensicaen.fr.

[e] Prof. Georgi N. Vayssilov,
Faculty of Chemistry and Pharmacy,
University of Sofia,
1126 Sofia, Bulgaria,
E-mail: gnv@chem.uni-sofia.bg.

[f] Prof. Valentin Valtchev,
Qingdao Institute of Bioenergy and Bioprocess Technology,
Chinese Academy of Sciences,
Qingdao, 266101, P. R. China,
E-mail: valentin.valtchev@ensicaen.fr.

Supporting information for this article is given via a link at the end of the document.

Abstract: The mesopores formation in zeolite crystals has long been considered to occur through the stochastic hydrolysis and removal of framework atoms. Here, we investigate the NH_4F etching of representative small, medium, and large pore zeolites and show that the zeolite dissolution behavior, therefore the mesopore formation probability, is dominated by zeolite architecture at both nano- and sub-nano scales. At the nano-scale, the hidden mosaics of zeolite structure predetermine the spatio-temporal dissolution of the framework, hence the size, shape, location, and orientation of the mesopores. At the sub-nano scale, the intrinsic micropore size and connectivity jointly determine the diffusivity of reactant and dissolved products. As a result, the dissolution propensity varies from removing small framework fragments to consuming nanodomains and up to full digestion of the outmost part of zeolite crystals. The new knowledge will lead to new understanding of zeolite dissolution behavior and new adapted strategies for tailoring hierarchical zeolites.

1. Introduction

Hierarchical zeolite, the materials with at least two pore size regimes, is definitely among the most important advances made in current porous materials science and technology.[1] It brings many new opportunities for the heterogeneous catalysis industry thanks to the greatly improved diffusion and accessibility.[2] In the past few decades, significant research efforts have been devoted to the continuous optimization of these technologically important materials, with the ultimate goal to achieve the tailored design. Steaming and/or acid leaching,[1a] alkaline treatment,[3] and fluoride medium etching[4] have successively emerged as representative dealumination (Al-biased), desilication (Si-biased), or dementalization (Al and Si unbiased) approaches for hierarchical zeolites engineering. A series of studies showing an important connection between framework defects and zeolite dissolution behavior has also been established.[5]

Despite these proven approaches and guiding principles, however, the cause, nature, and result of the "selected-area" dissolution have yet to be explored and rationalized in more detail. The formation and propagation of various mesopores in morphology, size, amount, spatiotemporal distribution, and connectivity is still not fully understood.[5b] In particular, several important questions remain to be answered (i) why do we get mesopores inside zeolite volume instead of dissolving the crystals completely; (ii) how we can rationalize the formation of mesopores with diversified pore size, density, and morphology in zeolites of different topologies after the same type of treatment; (iii) which factors dominate the different dissolution behavior of zeolites; and finally, (iv) whether some simple and generalized rules for explaining and predicting the dissolution behavior of a given zeolite can be formulated?

To address these issues, we decided to carry out an extensive study on the dissolution behavior of a variety of zeolites subjected to NH_4F etching. Dissolution in an ammonium fluoride medium is a non-traditional approach that offers a route to identify defects or irregularities in crystals that form during growth, i.e., the chemical bonds that break first would correspond to the weak bonds in the crystal.[4, 6] By using MFI-type zeolites as a model material, we have employed NH_4F etching to uncover defects of different types, corresponding to their concentration and spatial distribution, that are dependent upon the growth process.[7] Since the memory of the crystallization pathway(s) is coded in the crystal, the track of the dissolution pattern enables the recovery of a zeolite's growth history. Using a combination of complementary physicochemical techniques, we also identified the origin of the reported but not well-understood phenomena of zonal growth (defect-zoning and Al-zoning) in zeolites.[7b] These established experimental data show that studying dissolution reactions can be used as a powerful tool to reveal nucleation and crystal growth processes down to the atomic level and to obtain valuable information, which is not available by other methods.[7a]

In the present work, we further explore the advantage of NH_4F etching to understand the fundamentals of the hydrolysis of framework Si-O-Si(Al) bonds leading to mesopore formation in zeolites of varied framework topology. The Si and Al unbiased feature of NH_4F treatment make it uniquely possible to dissolve all zeolites with a single treatment and compare the products. This differs from the vast majority of processes reported in literature where the biased dissolution of framework atoms has been used.[8] Herein, the treatment of MFI, FAU, TON, and LTA type zeolites widely varied in Si and Al compositions, micropore size dimensions, and crystal topology are integrated and linked to each other.

2. Results and Discussion

2.1 The dissolution behavior of Silicalite-1

Silicalite-1 zeolite synthesized in F^- medium (S1-F) was the first to be treated. This is a 3D medium pore zeolite (Figure 1e-g) free of framework Al atoms. The scheduled treatment results in an obviously inhomogeneous dissolution pattern (Figure S1). A closer look at the dissolved parts reveals that the etching pits are very regular in shape (diamond-like in *b* face, rectangular in *a*) and a similar orientation (Figures 1a,b and S1b,d). Based on our previous research,[4, 7a], we attributed these well-defined domains to the removal of nanodomains hidden inside zeolite crystals. These mosaic domains are densely packed, overlapping with one another (Figure 1a).

Silicalite-1 zeolite synthesized in OH^- medium (S1-OH) was also treated and heavily dissolved in fluoride medium (Figure S2). The NH_4F etching revealed clearly the presence of "hour-glass" substructures in zeolite crystals (Figures 1c and S3). This shows that such substructures exist not only in very large crystals,[9] but also in zeolites of only a few microns. A close check of each substructure further revealed the presence of "mosaic structures" (Figure 1d), noting that the domain size is about 10 times smaller than what is shown in Figure 1a,b. Thus this part of the work shows that the mosaic domains are ubiquitously present in ZSM-5[4] and Silicalite-1 zeolites synthesized in both OH^- and F^- media (Figure 1), and in many other types of zeolites and zeotypes.[5d, 10] Apparently, the mosaic structures are a basic property of these zeolites and zeotypes. The hidden nanocrystalline domains are preferentially removed in a fluoride etching medium, leaving a very porous structure behind (Figure 1a-d).

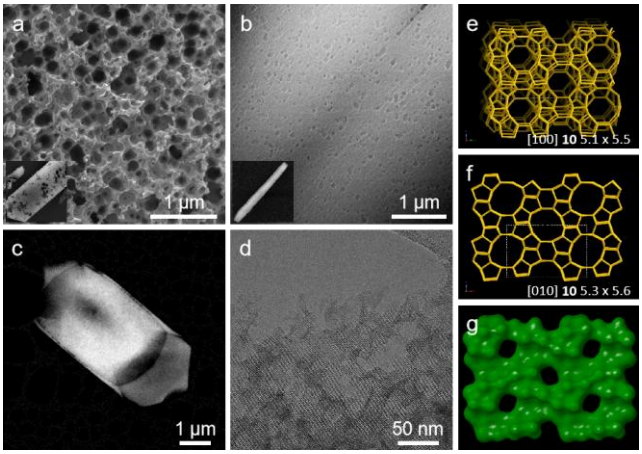

Figure 1. (a, b) SEM images showing the [100] (a) and [010] (b) crystal facets of the NH_4F treated Silicalite-1 zeolite synthesized in F^- medium (S1-F). (c, d) TEM images of the NH_4F treated Silicalite-1 zeolite synthesized in OH^- medium (S1-OH). (e, f) The framework images of MFI type zeolite viewed along [100] (e) and [010] (f), the corresponding pore size of the micropores are indicated in the image (the same bellow). (g) The 3D drawing of the cross-sections of the crossed straight and sinusoidal channels. All the framework images and 3D drawings are taken from the official website of the international zeolite association.[11]

2.2 The dissolution behavior of ZSM-22

ZSM-22 is a TON-type zeolite with a 1D medium pore system (Figure 2c,d). It is known in ZSM-22 synthesis, the zeolite formation includes the formation of isolated nanorods possessing the ZSM-22 characteristic; then, nanorods align and fuse through their lateral surfaces.[12] Mismatching interfaces and/or occluded intra-particle voids can naturally be expected if the assembly of the nanorods is not perfect. Then, according to our previous experience, the dissolution of such crystals in NH_4F solution should start preferentially from the imperfections, and the nanorods be preferentially removed. To test this conjecture, the NH_4F etching of ZSM-22 was conducted.

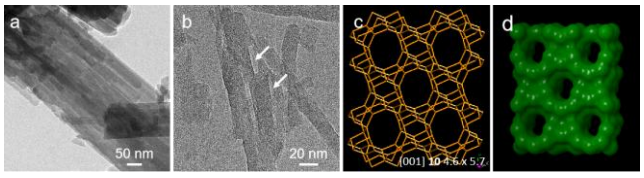

Figure 2. (a, b) TEM images of the parent (a) and NH_4F treated (b) ZSM-22 zeolites. The white arrows in (b) point to the empty space left by removing nano-rods. (c) The framework image of TON type zeolite viewed along [001]; (d) The 3D drawing of the cross-sections of the 1D straight channel.

The TEM images of the parent ZSM-22 used in the present work are shown in Figures 2a and S4. The periphery of some

nanorods is clearly distinguishable, being a clear sign that these nanorods are not perfectly aligned and coalesced with the main crystal. This particular growth results in the formation of some occluded mesoporous voids (Figure S4). The presence of occluded voids in the parent ZSM-22 was confirmed by the N_2 physisorption result (Figure S5). The pore size distribution (PSD) curve of the parent sample derived from the desorption branch of the isotherm exhibits a distinct peak at ca. 4 nm (Figure S5b). This is a clear sign for mesopores with a restricted connection to the external surface.[13] The applied fluoride etching results in the disassembly and segmentation of the ZSM-22 crystals. The zeolite morphology changes substantially from a bundled shape to needle-like single crystals (Figures 2a,b and S6). The treated samples remain highly crystalline (Figure S7) and microporous, while the mesopore volume increases continuously with the extension of NH_4F etching (Table S1). About 4 times higher mesopore volume was obtained after 45 min of treatment.

Despite the substantially increased mesopore volume, none of the treated samples shows the presence of occluded intra-particle mesoporosity (Figures S5 and S8). Only a few elongated mesopores penetrate in the volume of heavily dissolved crystals (Figure 2b). The substantially increased mesoporosity is related to the small size of the dissolved crystals (Figures S5 and S8). Correspondingly, there is no abrupt closure of isotherms at P/P_0=0.42 in the desorption branch (Figure S5a). The corresponding PSD curves do not show any peak at ca. 4 nm, in sharp contrast to the parent ZSM-22 (Figure S5b). The Si/Al ratio of the NH_4F treated ZSM-22 increases systematically with etching time (Table S2). There are no extra-framework species present, even for the most severely treated sample (Figure S9). It was reported that, in the synthesis of ZSM-22 zeolite, Al is inclined to be wrapped in the mantle of the nanorods during the fusion process.[12] Therefore, the continuously increased framework Si/Al ratios, combined with the absence of occluded secondary porosity, serve as strong evidence that there is no preferential dissolution of the nanorods embedded inside the bundled crystals. Contrariwise, substantial dissolution of zeolite framework happens, starting from the crystal periphery and advancing inward.

2.3 The dissolution behavior of zeolite A and zeolite X

In the following, we detail a comparative study of the NH_4F etching of zeolite X (FAU type, Figure 3b,c) and zeolite A (LTA type, Figure 3e,f). These two zeolites share the same secondary structure building units (sodalite cage, SOD) and the studied samples have a very similar Si/Al ratio (zeolite A: 1.1, Zeolite X: 1.4). However, they are very different in pore size dimensions. The framework of FAU is obtained when SODs are linked through double 6-rings (Figure 3b). This results in the formation of 12-ring large pores with a pore opening of 7.35 Å.[11] The 3D framework of LTA is obtained when SODs are linked through double 4-rings (Figure 3e). This results in the formation of 8-ring small pores with an opening of about 4.21 × 4.21 $Å^2$.[11]

The NH_4-form zeolite X was treated by NH_4F solutions of a broad concentration (Supporting information). The applied NH_4F treatment did not change the Si/Al ratio and macroscopic morphology of zeolite X even after the most severe fluoride etching with a 16 wt% aqueous NH_4F solution (Figure S10). The microporosity (Table S2) and crystallinity (Figure S11) of the NH_4F treated samples are gradually decreased along with the increased NH_4F concentration. On the other hand, the gradually enhanced NH_4F etching leads to a series of hierarchical zeolites (FX series, Figure 4a) with a continuously increased external surface and secondary pore volume (Table S2). The size of the mesopores estimated by using nitrogen physisorption is always centered at ca. 3–4 nm (Figure 4a). These small mesopores are homogeneously distributed throughout the FX zeolite crystals (Figure 3a). This dissolution behavior is very similar to that of zeolite Y in NH_4F solutions, noting that neither of them shows the presence of mosaic-shaped mesopores after fluoride etching.[6]

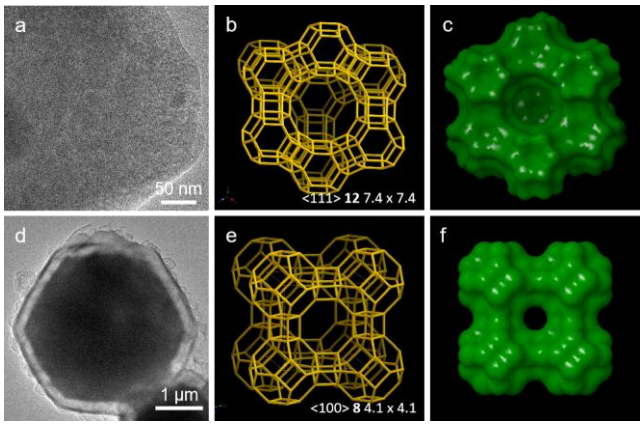

Figure 3. (a) TEM image of the NH_4F treated zeolite X. (b) The framework image of FAU type zeolite viewed along [111]. (c) The 3D drawing of the 12-ring large pore opening and the 3D connection of the micropores of zeolite X. (d) TEM image of NH_4F treated zeolite A showing the presence of a distinct ring surrounding a denser core of zeolite A. (e) The framework image of LAT type zeolite viewed along [100]. (f) The 3D drawing of the 8-ring small pore opening and the 3D connection of the micropores of zeolite A.

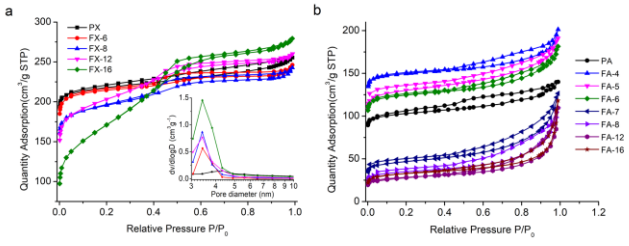

Figure 4. (a) The N_2 physisorption isotherms of the parent and NH_4F treated FAU-X type zeolites. The insert in Figure 4(a) shows the corresponding mesopore size distribution derived from the adsorption branch of the isotherms. (b) The N_2 physisorption isotherms of the parent and NH_4F treated LTA-type zeolites. The number suffix shows the NH_4F concentration (in wt%) used for the fluoride etching of the corresponding sample.

A similar yet even wider screening of the NH_4F etching conditions was carried on zeolite A (Supporting information). The NH_4F etching resulted in a substantial change of the surface morphology of zeolite A, in contrast to zeoliteX, even in the case of FA-4, the sample subjected to mildest etching (Figure S13-14). The characteristic diffraction peaks of the NH_4F treated samples

were largely retained (Figure S12). However, the surface of zeolite is covered by many sub-micron-sized particles (Figure S14-15), most probably fluorosilicate (aluminate) species. A careful inspection of the dissolved crystals' surface by high-resolution SEM reveals a clear layer-by-layer etching model (Figures S15). There is no sign of intra-particle mesopore formation. Thus, the formation of a hysteresis loop in nitrogen physisorption isotherms is attributed to the interstitial voids formed by the amorphous aggregates on zeolite surface. TEM study was applied on selected sample, and it revealed a unique ring-shaped shell surrounding a much denser core in the case of FA-16 (Figure 3d). Noteworthy is that the thickness of the shell is very homogeneous on every facet of the observed particle. The core part shows a homogeneous contrast indicating the absence of mesoporosity.

2.4 Dissolution behavior of zeolites: the impact of hidden mosaic structures and zeolite microporosity

Based on the results shown above, it is interesting to recall the surprising coincidence between NH_4F etching and alkaline treatment, a Si-selective chemical treatment,[14] in the post-synthesis engineering of zeolite mesoporosity. Specifically, both NH_4F and alkaline treatment result in hierarchical ZSM-5 zeolites with a typical mesopore size of around 10~20 nm.[4, 14] Both methods produce FAUtype hierarchical zeolites with a mesopore size of about 3 nm (Figure 4 and reference 15). On the other hand, the application of both alkaline leaching[16] and NH_4F etching to ZSM-22 fail to introduce intra-particle mesopores, but generate mainly a few surface etching pits (Figure 2 and Figure S8). Noting that the Si/Al ratio of both parent USY (Si/Al = 28.4[15]) and ZSM-22 (Si/Al = 42[16]) zeolites falls into the optimum range of 25–50 identified for the application of caustic etching.[3] As an insight into these regularities, the chemical etching of the same zeolite with NH_4F and NaOH of very different etching selectivity results in hierarchical zeolites with similar mesopore size and density. On the other hand, the chemical etching of different zeolite frameworks (MFI, TON, FAU, LTA) with the same etchant results in hierarchical zeolites of different mesopore size, density, and morphology. The intriguing observations documented in the literature and reported in the present study raise the general question of what determines a particular zeolite framework's dissolution behavior leading to mesopore formation.

A. The impact of hidden mosaic structure

We have shown that the appearance of the mosaic structure in zeolite crystals is inherently related to the multiple nucleation events during zeolite crystallization. In zeolite synthesis, the independent nuclei evolve into nanocrystalline domains through the addition of low-weight silica species or pre-formed 3D particles.[17] Meanwhile, these nanodomains merge and form the apparent single zeolite crystal in the end. An imperfect alignment of the nanodomains will produce strained boundaries rich in weak bonds. In principle, these chemical bonds will break first under chemical attack. Based on this understanding, a simple law of universal adaptability can be formulated for explaining and predicting the dissolution behavior of zeolites. Namely, the complete or incomplete dissolution of the hidden mosaic structure, starting from the defect-rich parts along the high-energy boundary, is intrinsically responsible for the zoned dissolution of zeolite crystals and the resultant secondary pore formation.

For the NH_4F treated MFI type zeolites, recognizing such a zoned dissolution behavior is straightforward, thanks to the sufficient removal of the hidden nano domains due to the Si and Al unbiased etching in NH_4F solution. Accordingly, the resultant secondary pores are impressively regular in morphology and orientation (Figure 1). The size of the secondary pores varies, as the size of the mosaic structure varies widely depending on the different crystallization rates under evolving supersaturation (Figure 1). These data further prove that the dissolution behavior and the resultant porous profile is predetermined by the inner architecture of zeolite crystals.[4, 7]

This preferential dissolution model is also appropriate in explaining why we can introduce mesopores into zeolite volume by alkaline treatment, bringing a new understanding for zeolite crystallization and dissolution mechanisms. In this case, the irregular profile of the mesopore morphology and orientation can be related to the incomplete removal of the hidden nanocrystalline domains, which is the result of the preferential removal of Si and/or the redeposition of the amorphous aluminosilicate species extracted from zeolite framework. We believe this zoned dissolution model is a better alternative than the protecting role of Aluminium in interpreting the pore size and spatial distribution of mesopores in alkaline treated zeolites.[3]

However, sometimes both alkaline treatment and fluoride etching fail to introduce intra-particle mesopores, although there is a mosaic-like structure presenting in zeolite crystals (Figure 2a). Besides, the preferential removal model is inadequate in interpreting the mesopore size and morphology of the alkaline or NH_4F treated FAUtype zeolite. For this large-pore zeolite with a 3D large pore system (Figure 3b,c), the chemical etching results in the formation of irregular-shaped mesopores with pore sizes much smaller than what has been observed in the case of ZSM-5 zeolite (Figure 1 and Figur 3a). Based on the established mechanism of crystallization by particle attachment[18] and the observation of diamond-shaped mesopores in FAU type zeolite[19], we believe that there are also mosaic structures presenting in this type of zeolite. It is, therefore, clear that the hidden mosaic structure is not the single factor for the inference of the consequent size, morphology, distribution, and orientation of chemical etching-induced mesopores.

B. The impact of zeolite microporosity

Based on the data shown above, we can see that the dissolution behavior of zeolite A in NH_4F solution sharply contrasts that of zeolite X. Comparing the many similarities and the only difference between these two zeolites leads to the conclusion that microporosity must be the critical factor responsible for the substantially different dissolution behavior. Namely, the pore size of zeolite A may be too small to allow the efficient diffusion of active fluoride species into crystal volume. As a result, the dissolution of zeolite A is mainly limited to the crystal periphery. This is supported by the N_2 physisorption data of the NH_4F treated zeolite A samples. One can easily notice that

the N_2 physisorption capacity of the FA-x series in the relative pressure range lower than 0.1 changes systematically with the NH_4F treatment conditions (Figure 4b). Specifically, the micropore volume accessible to N_2 probe molecules increased at first and then decreased dramatically (Table S2), as the concentration of NH_4F solutions increased from 4 wt% to 16 wt%. An increase in NH_4F concentration indicates a promoted hydrolysis and an increased formation of fluoride species active for Si and Al removal. As a result, the surface layer of zeolite A is progressively etched and evolved, first forming a surface layer with opened micropores and enhanced accessibility, and then covered and blocked by an increasing amount of amorphous species. Since the zeolite A is terminated all around with [100] facets, the dissolution front advances, and surface deposition happens, at a similar rate on each crystal face during fluoride etching. This accounts for the homogeneous ring-shaped surface dissolution (Figure 3d). Our conclusions on factors controlling zeolite A dissolution are in line with the data reported on another small pore zeolite (CHA-type).[10]

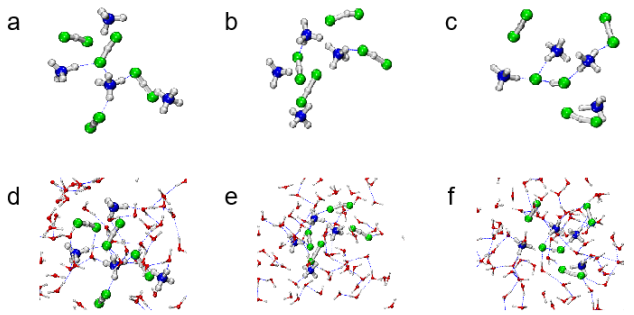

Figure 5. (a-c) Snapshots from the simulations with four $[HF_2]^-$ and four $[NH_4]^+$ moieties showing only ionic species. (d-f) Their location inside the solvent. Color coding: F– green; N – blue; O – red; H – white; H-bonds – blue dashed lines.

Retrospectively, the significant impact of micropore size on dissolution behavior was also reflected by the dissolution behavior of ZSM-22 in NH_4F solution. Namely, it was the limited diffusion inside the micropores of 1D medium-sized zeolite that obstructed the preferential dissolution of the crystal interior. As a result, the dissolution behavior of ZSM-22 in NH_4F solution is quite different from that of the MFI type zeolites, although the former zeolite also has mosaic-like domains in the crystals.

Besides the speculation made based on the visualized experimental data shown above, a solid knowledge of the size and geometry of the active species in the etchant can be very helpful for understanding the diffusion-controlled dissolution behavior. *Ab initio* molecular dynamics was further applied for simulating the geometry of fluoride species possibly existing in a reacting NH_4F medium (Figures 5 and S16-18). For this purpose, NH_4-HF_2 solution with different NH_3 : HF ratios was designed to represent the ever-evolving fluoride solution in contact with zeolite crystals.[4] The simulations with four $[HF_2]^-$ and four $[NH_4]^+$ moieties for 15-20 ps are shown in Figure 5. The modeling results show a group of complex and diversified fluoride moieties, including the NH_4F species, NH_4HF_2, $NH_4(HF_2)_2$, and many others. Both $[HF_2]^-$ and $[NH_4]^+$ moieties remain stable in part of the time, forming hydrogen bonds between the proton from the ammonium ion and a fluoride anion. However, both types of species form more hydrogen bonds with the solvating water molecules, and some of them are completely solvated by water without interaction with the counter ion. This can be seen in the snapshots from the simulations showing only ionic species (Figure 5a-c) and their location inside the solvent (Figure 5d-f). Our simulations have also shown that the formation of NH_4HF_2 complex is energetically favorable over the separately solvated ionic moieties (see Figure S17 and corresponding discussion in SI).

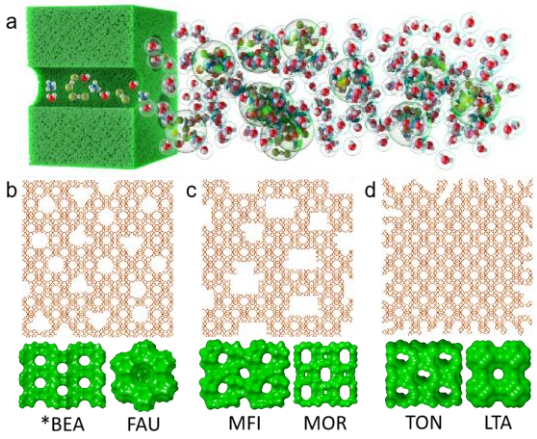

Figure 6. (a) Schematics of zeolite – fluoride interactions at the interface between crystal surface and NH_4F solution. The dissolution behavior of zeolites in NH_4F solution depends on the intrinsic microporosity of zeolite crystals. (b) Small, ill-defined mesopores in 3D large pore zeolite FAU. (c) Large regular mesopores in 3D medium pore and 1D large pore zeolites MFI and MOR. (d) Localized and intensive surface etching in 1D medium pore and 3D small pore zeolites TON and LTA.

Some of these species, especially the most active ones for Si and Al removal,[20] are clustered or solvated via hydrogen bonds, forming bulky spherical moieties that may be difficult to enter the small-size (8MR) pores (Figure 6a).[21] This is because the chemical etching process involves a substantial exchange of matter, including diffusion in and out of reactant species and etching products, respectively, via molecule diffusion, which is further complicated by the ongoing chemical reactions at the solid-liquid interface.[21] The simultaneous progress of all these events in microporous materials is spatially demanding. Such pore size effects in zeolite dissolution have some in common with gas adsorption and catalytic reactions in zeolite micropores.[22] In all cases, the molecule motion is strongly influenced by the exact size, shape, and dimensions of the micropore channels.

Following this line of reasoning, the experimentally observed data can be interpreted as follows. Apparently, the large 12-rings and the three-dimensional channel system (*BEA, FAU) favor fast diffusion of etchant and etched products. As a result, the dissolution of zeolites with a very open pore system does not follow a reverse layer-by-layer mechanism [23] but starts homogeneously from the microporous walls inside crystals instead (Figure 6b).[24] As a result, it allows a fine-tuning of zeolite porosity, especially when there is hidden micropore volume in zeolite framework to be explored (such as SOD cages in Figure 3).[5d, 6, 24] For medium pore-sized zeolites with multi-dimensional channels, such as MFI type structures, the hidden mosaic domains are preferentially removed (Figure 6c) without an intermediate enhancement of the micropore

volume.[23] Mordenite also has a large 12-rings pore system, but the 1D channel is very unfavorable for intra-particle diffusion.[5d, 25] As a result, the dissolution of mordenite in NH_4F follows the reverse layer-by-layer mechanism, similar to the MFI type zeolites.[5d] In the end, zeolites with severely restricted intraparticle diffusivity show no sign of preferential removal of the crystal interior (Figure 6d), as the active fluoride species are too bulky to enter the inner part of zeolite crystals. With a continuous increase of NH_4F in concentration, the fast kinetics of surface etching will overcome the relatively slower intracrystalline. Conseqeuntly, the intensive dissolution of zeolite crystal is limited to the periphery (Figure 3d, Figure S14-15).

So far, we have shown above both experimental and computational results proving that the micropore size and dimensions of zeolites predetermine the diffusivity of reactant and dissolved products. Hence it plays an important role in determining the size, morphology, and distribution of generated mesopores. With this knowledge in mind, the dissolution behavior of other types of zeolites can be explained. For example, none of the previously published protocols succeeds in producing intra-particle mesopores inside LTA and CHA-type zeolites and zeotypes.[10a, 26] Obviously, this is because the dissolution of zeolite crystals is limited to the zeolite periphery or extended grain boundaries like the interface between macroscopic intergrowths.

Conclusion

In summary, the intrinsic reasons for diverse zeolite dissolution behavior, and therefore varied mesoporosity, have been discussed in detail. Hidden mosaic structures inherited from zeolite synthesis and the intrinsic microporosity properties of zeolites are identified as interlocking factors in shaping the final dissolution behavior of zeolite crystals and the resultant secondary porosity pattern. While the size, shape, concentration, and spatial distribution of the mosaic structure predefine the size and morphology of the generated space left by dissolution, the overall dissolution process is diffusion controlled. Namely, the dimensions and topology of the micropores determine the dissolution preference towards single framework atoms, interior mosaic blocks, or exterior features of zeolite crystals. Therefore, although the mosaic structure is a common feature of zeolite crystals, transforming the intimate crystal structure into visible mesoporosity is not straightforward since theframework dissolution behavior depends also on zeolite microporosity.

Acknowledgments

Z.Q. acknowledges the support from NSFC21706285, Qingdao Applied Basic Research Project (19-6-2-70-cg), the Fundamental Research Funds for the Central Universities (18CX02013A); S.M. acknowledges the support from NSFC21975285 and Thousand Talents Program for Foreign Experts (WQ20152100316); Z.Q. and S.M. acknowledge the support from NSFC 21991090, NSFC21991091. Z.Q. S.M. and V.V. acknowledge the collaboration in the framework of joint Sino-French international laboratory “Zeolites”. GNV acknowledges the support from Bulgarian Ministry of Education and Science, contract D01-76/2021, and computational resources from Nestum facility of Sofia Tech park.

Keywords: Zeolites • NH_4F etching • Dissolution mechanism • Mesopore • Diffusion

[1] a) S. Van Donk, A. H. Janssen, J. H. Bitter, K. P. de Jong, *Catal Rev Sci Eng* **2003**, *45*, 297-319; b) J. Pérez-Ramírez, C. H. Christensen, K. Egeblad, C. H. Christensen, J. C. Groen, *Chem. Soc. Rev.* **2008**, *37*, 2530-2542; c) C. M. Parlett, K. Wilson, A. F. Lee, *Chem. Soc. Rev.* **2013**, *42*, 3876-3893; d) A. Feliczak-Guzik, *Microporous Mesoporous Mater.* **2018**, *259*, 33-45; e) J. D. Rimer, A. Chawla, T. T. Le, *Annual review of Chem. Bio. Eng.* **2018**, *9*, 283-309; f) M. Shamzhy, M. Opanasenko, P. Concepción, A. Martínez, *Chem. Soc. Rev.* **2019**, *48*, 1095-1149.

[2] a) M. Hartmann, *Angew. Chem. Int. Ed.* **2004**, *43*, 5880-5882; b) K. Li, J. Valla, J. Garcia-Martinez, *ChemCatChem* **2014**, *6*, 46-66; c) D. Schneider, D. Mehlhorn, P. Zeigermann, J. Kärger, R. Valiullin, *Chem. Soc. Rev.* **2016**, *45*, 3439-3467; d) V. Blay, B. Louis, R. n. Miravalles, T. Yokoi, K. A. Peccatiello, M. Clough, B. Yilmaz, *ACS Catal.* **2017**, *7*, 6542-6566.

[3] J. C. Groen, L. A. Peffer, J. A. Moulijn, J. Pérez‐Ramírez, *Chem. Eur. J.* **2005**, *11*, 4983-4994.

[4] Z. Qin, G. Melinte, J. P. Gilson, M. Jaber, K. Bozhilov, P. Boullay, S. Mintova, O. Ersen, V. Valtchev, *Angew. Chem. Int. Ed.* **2016**, *128*, 15273-15276.

[5] a) S. Svelle, L. Sommer, K. Barbera, P. Vennestrøm, U. Olsbye, *Catal. Today* **2011**, *168*, 38; b) S. Mitchell, A. B. Pinar, J. Kenvin, P. Crivelli, J. Kärger, J. Pérez-Ramírez, *Nat. Commun.* **2015**, *6*, 1-14; c) T. Li, J. Ihli, J. T. Wennmacher, F. Krumeich, J. A. van Bokhoven, *Chem. Eur. J.* **2019**, *25*, 7689-7694; d) Z. Qin, L. Hafiz, Y. Shen, S. Van Daele, P. Boullay, V. Ruaux, S. Mintova, J.-P. Gilson, V. Valtchev, *J. Mater. Chem. A* **2020**, *8*, 3621-3631.

[6] Z. Qin, K. A. Cychosz, G. Melinte, H. El Siblani, J.-P. Gilson, M. Thommes, C. Fernandez, S. Mintova, O. Ersen, V. Valtchev, *J. Am. Chem. Soc.* **2017**, *139*, 17273-17276.

[7] a) K. N. Bozhilov, T. T. Le, Z. Qin, T. Terlier, A. Palčić, J. D. Rimer, V. Valtchev, *Sci. Adv.* **2021**, *7*, eabg0454; b) Y. Shen, Z. Qin, S. Asahina, N. Asano, G. Zhang, S. Qian, Y. Ma, Z. Yan, X. Liu, S. Mintova, *J. Mater. Chem. A* **2021**, *9*, 4203-4212.

[8] a) R. L. Hartman, H. S. Fogler, *Langmuir* **2007**, *23*, 5477-5484; b) L. I. Meza, M. W. Anderson, B. Slater, J. R. Agger, *Phys. Chem. Chem. Phys.* **2008**, *10*, 5066-5076; c) R. Brent, P. Cubillas, S. M. Stevens, K. E. Jelfs, A. Umemura, J. T. Gebbie, B. Slater, O. Terasaki, M. A. Holden, M. W. Anderson, *J. Am. Chem. Soc.* **2010**, *132*, 13858-13868.

[9] F. C. Hendriks, J. E. Schmidt, J. A. Rombouts, K. Lammertsma, P. C. Bruijnincx, B. M. Weckhuysen, *Chem. Eur. J.* **2017**, *23*, 6305-6314.

[10] a) X. Chen, A. Vicente, Z. Qin, V. Ruaux, J.-P. Gilson, V. Valtchev, *ChemComm* **2016**, *52*, 3512-3515; b) K.-G. Haw, S. Moldovan, L. Tang, Z. Qin, Q. Fang, S. Qiu, V. Valtchev, Inorg. Chem. Front. **2020**, *7*, 2154-2159.

[11] https://asia.iza-structure.org/IZA-SC/ftc_table.php.

[12] K. Hayasaka, D. Liang, W. Huybrechts, B. R. De Waele, K. J. Houthoofd, P. Eloy, E. M. Gaigneaux, G. Van Tendeloo, J. W. Thybaut, G. B. Marin, *Chem. Eur. J.* **2007**, *13*, 10070-10077.

[13] J. Zečević, C. J. Gommes, H. Friedrich, P. E. de Jongh, K. P. de Jong, *Angew. Chem. Int. Ed.* **2012**, *51*, 4213-4217.

[14] D. Verboekend, J. Pérez‐Ramírez, *Chem. Eur. J.* **2011**, *17*, 1137-1147.

[15] a) K. P. De Jong, J. Zečević, H. Friedrich, P. E. De Jongh, M. Bulut, S. Van Donk, R. Kenmogne, A. Finiels, V. Hulea, F. Fajula, *Angew. Chem. Int. Ed.* **2010**, *49*, 10074-10078; b) T. Ennaert, J. Van Aelst, J. Dijkmans, R. De Clercq, W. Schutyser, M. Dusselier, D. Verboekend, B. F. Sels, *Chem. Soc. Rev.* **2016**, *45*, 584-611.

[16] D. Verboekend, A. M. Chabaneix, K. Thomas, J.-P. Gilson, J. Pérez-Ramírez, *CrystEngComm* **2011**, *13*, 3408-3416.

[17] A. I. Lupulescu, J. D. Rimer, *Science* **2014**, *344*, 729-732.

[18] a) J. J. De Yoreo, P. U. Gilbert, N. A. Sommerdijk, R. L. Penn, S. Whitelam, D. Joester, H. Zhang, J. D. Rimer, A. Navrotsky, J. F.

Banfield, *Science* **2015**, *349*; b) G. Mirabello, A. Ianiro, P. H. Bomans, T. Yoda, A. Arakaki, H. Friedrich, G. de With, N. A. Sommerdijk, Nat. Mater. **2020**, *19*, 391-396.

[19] H. Ajot, J. Joly, J. Lynch, F. Raatz, P. Caullet, *Stud Surf Sci Catal* **1991**, pp. 583-590.

[20] Z. Qin, L. Lakiss, J.-P. Gilson, K. Thomas, J.-M. Goupil, C. Fernandez, V. Valtchev, *Chem. Mater.* **2013**, *25*, 2759-2766.

[21] G. Daccord, *Phys. Rev. Lett.* **1987**, *58*, 479.

[22] Y. Traa, J. Weitkamp, *Handbook of Porous Solids* **2002**, 1015-1057.

[23] Z. Qin, L. Pinard, M. A. Benghalem, T. J. Daou, G. Melinte, O. Ersen, S. Asahina, J.-P. Gilson, V. Valtchev, *Chem. Mater.* **2019**, *31*, 4639-4648.

[24] Z. Qin, S. Zeng, G. Melinte, T. Bučko, M. Badawi, Y. Shen, J. P. Gilson, O. Ersen, Y. Wei, Z. Liu, *Adv. Sci.* **2021**, *8*, 2100001.

[25] J. Lourenço, M. Ribeiro, F. R. Ribeiro, J. Rocha, Z. Gabelica, Appl. Catal. A **1996**, *148*, 167-180.

[26] a) D. Verboekend, T. C. Keller, S. Mitchell, J. Pérez‐Ramírez, *Adv. Funct. Mater.* **2013**, *23*, 1923-1934; b) D. Verboekend, M. Milina, J. Perez-Ramirez, *Chem. Mater.* **2014**, *26*, 4552-4562.

Entry for the Table of Contents

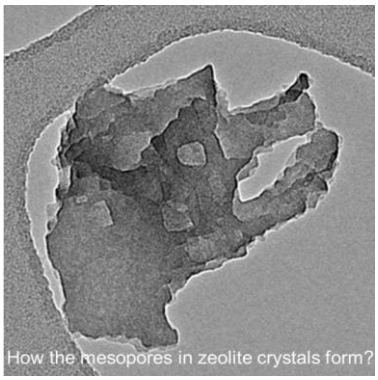

The particularities of zeolites dissolution topology provide important insights into long-standing questions about the mechanisms leading to mesopore formation.